

Antenna Linear-Quadratic-Gaussian (LQG) Controllers: Properties, Limits of Performance, and Tuning Procedure

W. Gawronski¹

Wind gusts are the main disturbances that depreciate tracking precision of microwave antennas and radiotelescopes. The linear-quadratic-Gaussian (LQG) controllers—as compared with the proportional-and-integral (PI) controllers—significantly improve the tracking precision in wind disturbances. However, their properties have not been satisfactorily understood; consequently, their tuning is a trial-and-error process. A control engineer has two tools to tune an LQG controller: the choice of coordinate system of the controller model and the selection of weights of the LQG performance index. This article analyzes properties of an open- and closed-loop antenna. It shows that the proper choice of coordinates of the open-loop model simplifies the shaping of the closed-loop performance. The closed-loop properties are influenced by the LQG weights. The article shows the impact of the weights on the antenna closed-loop bandwidth, disturbance rejection properties, and antenna acceleration. The bandwidth and the disturbance rejection characterize the antenna performance, while the acceleration represents the performance limit set by the antenna hardware (motors). The article presents the controller tuning procedure, based on the coordinate selection and the weight properties. The procedure rationally shapes the closed-loop performance, as an alternative to the trial-and-error approach.

I. Problem Statement

The pointing and tracking requirements are increasingly stringent for new and existing antennas and radiotelescopes. For example, communication at 32 GHz (Ka-band) for NASA's Deep Space Network (DSN) antennas requires pointing accuracy of 1 mdeg (rms) [1,2]; the Large Millimeter Telescope (LMT) built at Cerro La Negra, Mexico, by the University of Massachusetts and Instituto Nacional de Astrofísica, Óptica y Electrónica, requires pointing of 0.3 mdeg (see [3]). These requirements forced the implementation of the linear-quadratic-Gaussian (LQG) controllers. The control system of the 34-m DSN antenna shown in Fig. 1 includes the LQG algorithm. It meets the Ka-band requirements and was used to track the Cassini spacecraft on its journey to Saturn. This article presents principles of the LQG controller design, allowing for shaping of the tracking and disturbance rejection properties of antennas or radiotelescopes.

¹ Communications Ground Systems Section.

The research described in this publication was carried out by the Jet Propulsion Laboratory, California Institute of Technology, under a contract with the National Aeronautics and Space Administration.



Fig. 1. The 34-m NASA/JPL DSN antenna at Goldstone, California.

The tuning of LQG controllers used for antenna tracking purposes is a tricky process. The controller addresses the antenna tracking requirements (such as minimization of antenna servo error in wind gusts and fast response to commands) and the antenna limitations (such as acceleration limits and dependence on motor size). The LQG closed-loop properties are defined through the LQG performance index, which is shaped by parameters called LQG weights. The requirements, however, are not directly reflected in the LQG weights. Thus, the relationship between LQG weights (controller design tools) and antenna requirements needs to be established. This article answers this question indirectly. It explains the properties of a simple (proportional-and-integral, PI) controller and a simple (rigid) antenna, and next, by analogy, extends these properties—under certain conditions—to a real antenna with an LQG controller. This connection leads to the development of a controller tuning method that addresses the antenna tracking performance criteria.

The antenna controller tuning procedure introduced in this article is developed in three steps: the adjustment of the open-loop model (through selection of the coordinate system and auxiliary components), the analysis of a simple (rigid) antenna and simple (PI) controller (to derive basic properties of the closed-loop system), and, finally, the extension of the properties of a simple system to the real (flexible) antenna and a complex (LQG) controller.

II. Open-Loop Model

The antenna control system typically monitors two axes of motion, the azimuth and elevation axes. Since motions in both axes are uncoupled, in the following only a single axis is analyzed.

The antenna control system is shown in Fig. 2. It consists of the antenna open-loop system, position controller, and rate and acceleration limiters. The controller output u represents the commanded rate, and its derivative is the commanded acceleration, a .

In terms of hardware, an antenna open-loop system consists of the antenna structure, drives (motors, gears, and amplifiers), and the rate-loop feedback. The antenna position (measured at the encoder) is the output of the open-loop system. Antenna rate (as voltage or as a digital rate) is its input. The antenna open-loop model, shown in Fig. 3, is obtained (from field tests and the system identification) in the state-space form

$$\left. \begin{aligned} \dot{x} &= Ax + Bu + w \\ y &= Cx \end{aligned} \right\} \quad (1)$$

where x is the state, w is the disturbance, y is the antenna position, and (A, B, C) is the state-space triple.

The antenna open-loop model is used in the LQG controller design (it is a part of the LQG estimator). Thus, the accuracy of the model and its coordinate selection are the factors that influence the performance of the LQG controller. The accuracy is solved by determining the model through field testing of the open-loop antenna and system identification. The selection of coordinates is discussed in the following. The state-space model—obtained from system identification—is transformed into the coordinates convenient for the tuning of the antenna controller. The transformation consists of three stages:

- (1) Transformation to modal coordinates
- (2) Transformation to coordinates with the antenna position as the first state
- (3) Augmenting the model with the integral of the position

In the first step, the state-space model (A, B, C) given by Eq. (1) is transformed into the model (A_m, B_m, C_m) in modal coordinates, with the modal state vector x_m ; for details see [4]. The modal state-space representation is characterized by the block-diagonal state matrix, A_m , and by the weakly

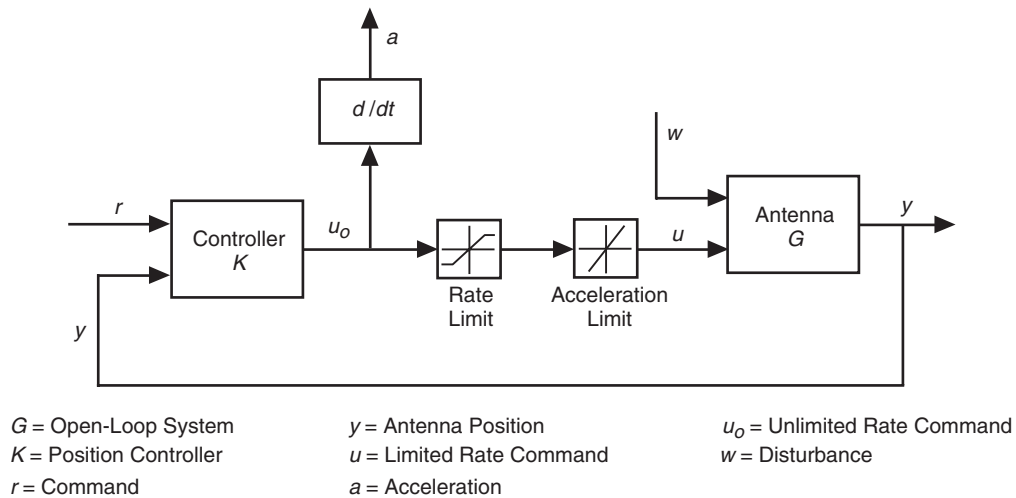


Fig. 2. Antenna control system.

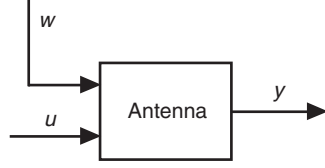


Fig. 3. Antenna open-loop system.

coupled modal states, $x_m^T = [x_{1m}^T, x_{2m}^T, \dots]$, where the i th component x_{im} is the state of the i th mode, $x_{im}^T = \{x_{i1m} \ x_{i2m}\}$. The weak coupling allows each modal state to be adjusted independently, which vastly simplifies the controller tuning process.

The modal model is transformed further in order to obtain the new state, x_p , with the first state the antenna position, while the remaining states are untouched (the antenna position is a controlled variable). Thus, the new state after transformation is as follows:

$$x_p = \begin{Bmatrix} y \\ x_f \end{Bmatrix} \quad (2)$$

where y is the antenna position, and x_f denotes the remaining (unchanged) states. The new state-space representation, (A_p, B_p, C_p) , is obtained using the following transformation:

$$x_p = P x_m \quad (3)$$

where, for n states, we have

$$P = \begin{bmatrix} C_{m1} & C_{m2} \\ 0_{n-1,1} & I_{n-1} \end{bmatrix} \quad (4)$$

($0_{n-1,1}$ is the zero vector $(n-1) \times 1$, and I_{n-1} is the identity matrix of order $n-1$.) The transformation was derived by noting that $y = C_m x_m$, and dividing C_m as follows: $C_m = [C_{m1} \ C_{m2}]$, where C_{m1} is the first component of C_m , and C_{m2} represents the remaining components.

Next, the model is augmented with an integrator, as recommended in [5–7], to eliminate the steady-state errors in constant-rate tracking and to improve the antenna disturbance rejection properties. Thus, the integral of the position (denoted y_i) is added to the state-space model as a new state, obtaining the state x_o :

$$x_o = \begin{Bmatrix} y_i \\ x_p \end{Bmatrix} = \begin{Bmatrix} y_i \\ y \\ x_f \end{Bmatrix} \quad (5)$$

The new state y_i satisfies the following equation:

$$\dot{y}_i = y = C_p x_p \quad (6)$$

and is added to the state-space representation, (A_p, B_p, C_p) , obtaining a new representation, (A_o, B_o, C_o) :

$$A_o = \begin{bmatrix} 0 & C_p \\ 0 & A_p \end{bmatrix}; \quad B_o = \begin{bmatrix} 0 \\ B_p \end{bmatrix}; \quad C_o = [0 \quad C_p] \quad (7)$$

The state x_o as in Eq. (5) is the desired state vector of the antenna open-loop system, and Eq. (7) is the preferred open-loop model of the antenna. The open-loop state consists of the integral of the position, the position, and the flexible deformations in modal coordinates.

The open-loop system hardware and software are designed such that they approximately represent an integrator, as shown in Fig. 4. The magnitude of the transfer function of a perfect integrator $1/s$ is shown in Fig. 4 (dashed line) as a straight line sloping at -20 dB/dec. The magnitude of the transfer function of the 34-m antenna obtained from field testing is shown in Fig. 4 (solid line) as a straight line sloping at -20 dB/dec for low frequencies (up to 1 Hz); it shows flexible deformations (resonances) at higher frequencies (structural and drive flexibility causes deformations that are not a part of integration).

III. PI Controller and a Rigid Antenna

The position controller of a rigid antenna is assumed to be a simple proportional-and integral (PI) controller, as shown in Fig. 5.

In the closed-loop system shown in Fig. 2, K denotes the controller transfer function and G is the antenna transfer function. A rigid antenna is a pure integrator; thus, for the PI controller and rigid antenna, we have

$$K = k_p + \frac{k_i}{s} \quad \text{and} \quad G = \frac{1}{s} \quad (8)$$

where k_p is the proportional gain and k_i is the integral gain. Also, in Fig. 2 r is a command, u is the controller output (called rate command), a is the commanded acceleration (a derivative of the controller input u), w is wind disturbance, y is the antenna angular position, and $e = r - y$ is a servo error.

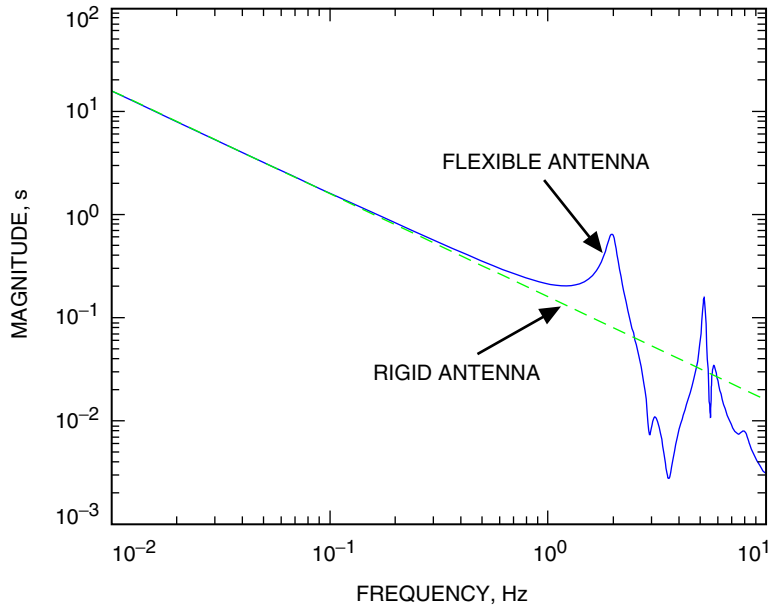


Fig. 4. Magnitudes of the transfer function of the open-loop model of the 34-m antenna (solid line) and a rigid antenna (dashed line).

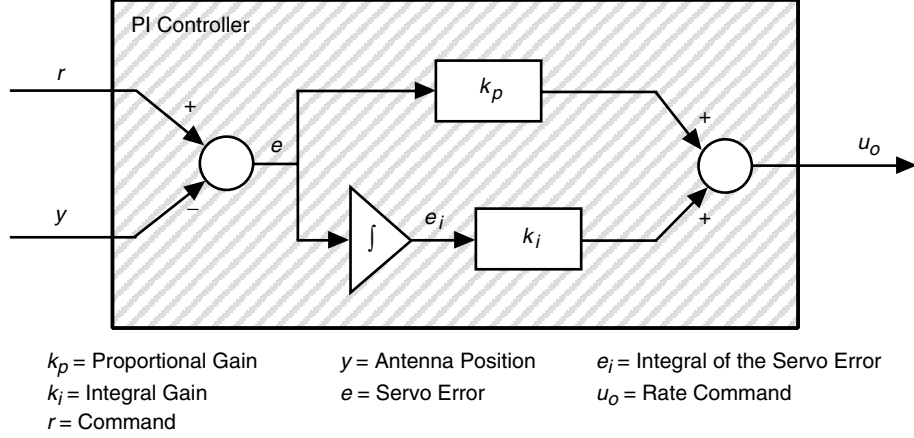


Fig. 5. PI controller.

A. Closed-Loop Transfer Functions

In order to explain the impact of the command r and disturbances w on the antenna position y and the commanded acceleration a , we analyze the following transfer functions: T_{ry} , from the command to the encoder; T_{wy} , from the disturbance to the encoder; T_{ra} , from the command to the acceleration; and T_{wa} , from the disturbance to the acceleration. From the block diagram in Fig. 2, we obtain

$$T_{ry} = \frac{GK}{1 + GK} \quad \text{and} \quad T_{wy} = \frac{G}{1 + GK} \quad (9)$$

$$T_{ra} = \frac{sK}{1 + KG} \quad \text{and} \quad T_{wa} = \frac{-sKG}{1 + KG} \quad (10)$$

and by introducing Eq. (8) to Eqs. (9) and (10), we get

$$T_{ry} = \frac{k_p s + k_i}{s^2 + k_p s + k_i} \quad \text{and} \quad T_{wy} = \frac{s}{s^2 + k_p s + k_i} \quad (11)$$

$$T_{ra} = \frac{(k_p s + k_i) s^2}{s^2 + k_p s + k_i} \quad \text{and} \quad T_{wa} = \frac{-(k_p s + k_i) s}{s^2 + k_p s + k_i} \quad (12)$$

B. The Proportional Gain Analysis

The controller tuning starts with the selection of the proportional gain; thus, we assume $k_i = 0$ in the above transfer functions [see Eqs. (11) and (12)], obtaining

$$T_{ry} = \frac{1}{\frac{1}{k_p} s + 1} \quad \text{and} \quad T_{wy} = \frac{1}{\frac{1}{k_p} s + 1} \quad (13)$$

$$T_{ra} = \frac{s^2}{\frac{1}{k_p}s + 1} \quad \text{and} \quad T_{wa} = \frac{-s}{\frac{1}{k_p}s + 1} \quad (14)$$

The magnitudes of the above transfer function are shown in Fig. 6. We see from this figure that the increase of the proportional gain

- (1) Increases the bandwidth of the transfer function T_{ry} (from the command to the antenna position); see Fig. 6(a)
- (2) Improves the disturbance rejection properties of the antenna by lowering the magnitude of the disturbance rejection transfer function T_{wy} ; see Fig. 6(b)
- (3) Increases the impact of the command on the antenna acceleration (increases the magnitude and the bandwidth of the acceleration transfer function T_{ra}); see Fig. 6(c)
- (4) Increases the impact of disturbances on the antenna acceleration (increases the magnitude and the bandwidth of the acceleration transfer function T_{wa}); see Fig. 6(d)

The first two transfer functions show the improvement of the antenna performance with the increase of the proportional gain. However, the last two show a potential problem: antenna acceleration increases at high frequencies, due both to command and to disturbances. The increased acceleration indicates that the antenna can hit the acceleration limit and enter a nonlinear regime; consequently, its performance will deteriorate, leading even to instability. Thus, the proportional gain increase is limited by the acceleration limits imposed at the antenna drives.

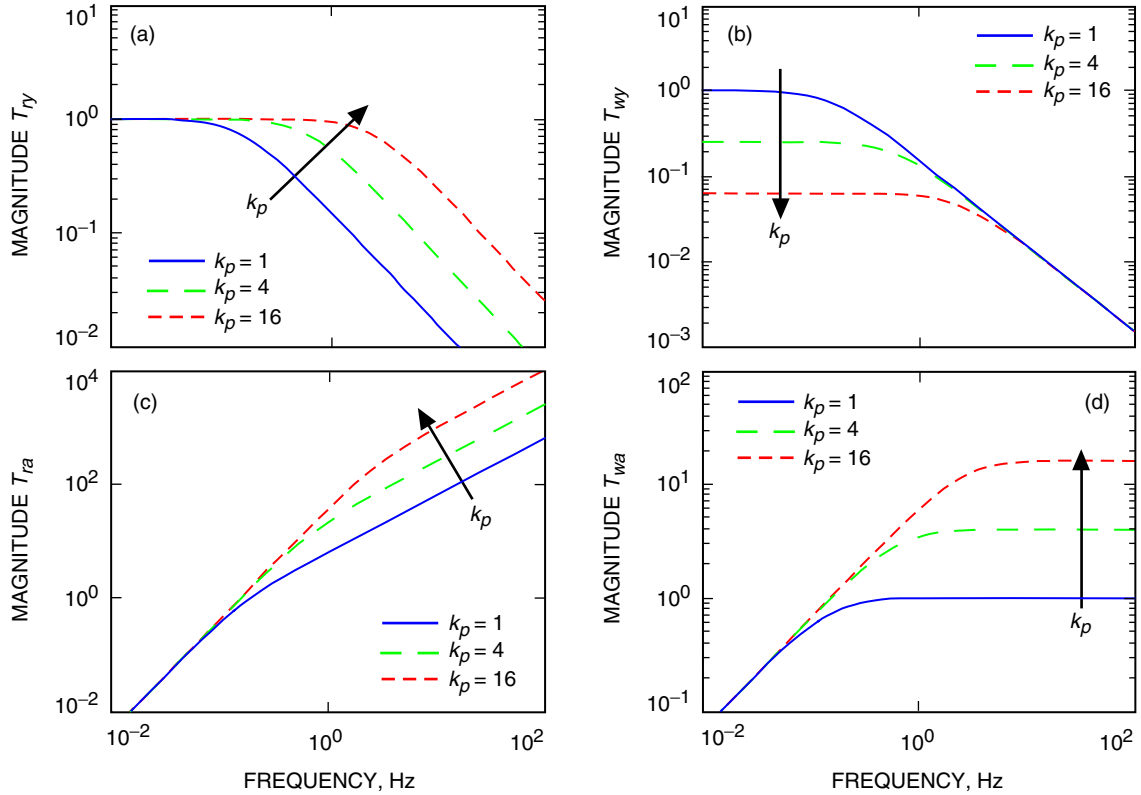


Fig. 6. Magnitudes of the transfer functions of the proportional controller, $k_i = 0$: (a) T_{ry} , from the command to the encoder, (b) T_{wy} , from the disturbance to the encoder, (c) T_{ra} , from the command to the acceleration, and (d) T_{wa} , from the disturbance to the acceleration.

C. The Integral Gain Analysis

Before we analyze the impact of the integral gain on antenna dynamics, we introduce two critical values: the critical integral gain and the critical frequency.

1. Critical Integral Gain. It is well known that large integral gain causes low-frequency oscillations of the closed-loop system. Consider the poles s_1 and s_2 of the closed-loop system, Eqs. (11) and (12), i.e., the roots of the polynomial $s^2 + k_p s + k_i$:

$$s_{1,2} = 0.5 \left(-k_p \pm \sqrt{k_p^2 - 4k_i} \right) \quad (15)$$

The system is non-oscillatory if poles are real, which happens when $k_p > 2\sqrt{k_i}$ or when

$$k_i \leq 0.25 k_p^2 \quad (16)$$

Thus,

$$k_{ic} = 0.25 k_p^2 \quad (17)$$

is the upper limit of the integral gain, called the critical integral gain.

2. Critical Frequency. For the critical integral gain, the denominator of the transfer functions shown in Eqs. (11) and (12) is as follows: $s^2 + k_p s + 0.25 k_p^2 = (s + 0.5 k_p)^2$. At frequency

$$\omega_o = 0.5 k_p = \sqrt{k_i} \quad (18)$$

the slope of the transfer function drops by -40 dB/dec. This is the critical frequency of the closed-loop system that determines the antenna bandwidth. In the following, the frequencies significantly smaller than ω_o are called low frequencies; frequencies significantly larger than ω_o are called high frequencies; and frequencies in the neighborhood of ω_o are called medium frequencies.

The following analysis shows how the transfer functions depend on the integral gain by considering low, medium, and high frequencies in Eqs. (11) and (12). Note first that for medium frequencies the variations of all four transfer functions are minimal (see Fig. 7) since the integral gain is smaller than the critical integral gain. For low and high frequencies, the transfer functions behave as follows:

- (1) The transfer function T_{ry} does not depend on k_i , since for low frequencies $T_{ry} \cong 1$ and for high frequencies $T_{ra} \cong k_p/s$, as shown in Fig. 7(a).
- (2) The transfer function T_{wy} is inverse proportional to k_i for low frequencies, since $T_{wy} \cong s/k_i$, and for high frequencies, it does not depend on k_i since $T_{wy} \cong 1/s$, as shown in Fig. 7(b).
- (3) The transfer function T_{ra} does not depend on k_i , since for low frequencies $T_{ra} \cong s^2$, and for high frequencies $T_{ra} \cong k_p s$, as shown in Fig. 7(c).
- (4) The transfer function T_{wa} does not depend on k_i , since for low frequencies $T_{wa} \cong -s$, and for high frequencies $T_{wa} \cong -k_p$, as shown in Fig. 7(d).

The above analysis showed that the integral gain impacts the disturbance rejection transfer function T_{wy} only, and that the impact is at low frequencies.

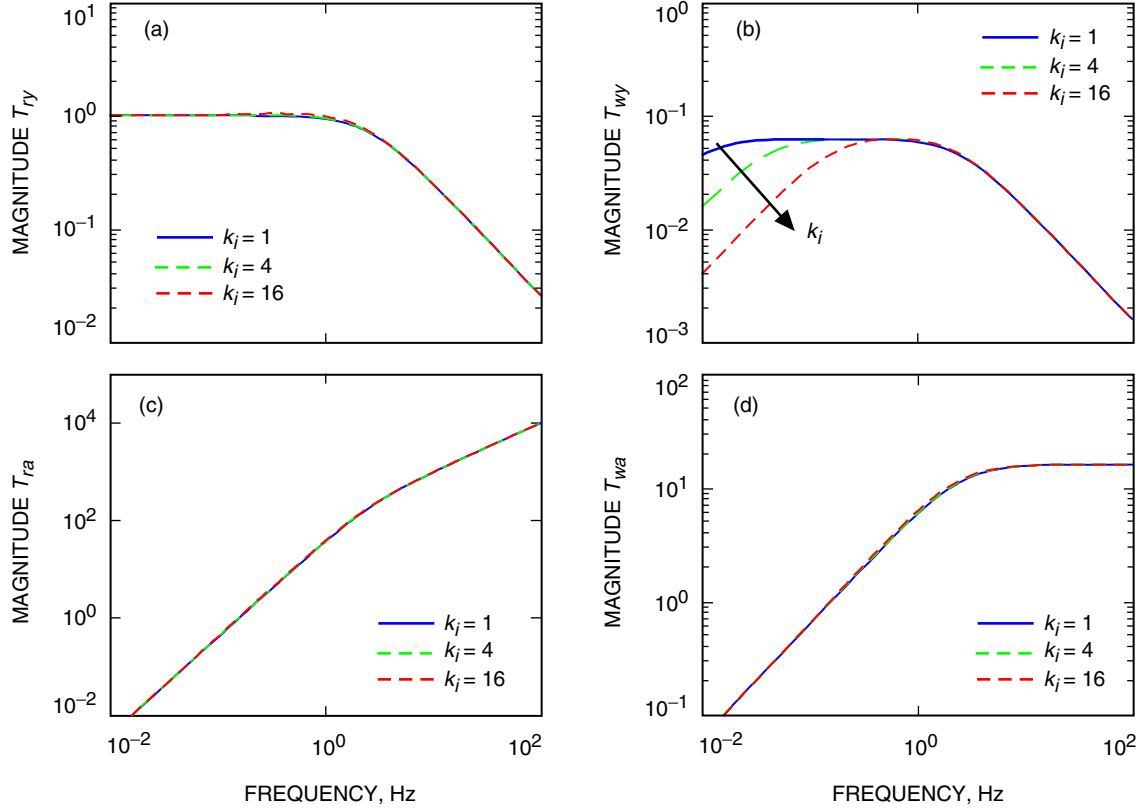


Fig. 7. Magnitudes of the transfer functions of the PI controller, $k_p = 16$: (a) T_{ry} , (b) T_{wy} , (c) T_{ra} , and (d) T_{wa} .

D. PI Controller Tuning Procedure

The PI controller tuning procedure involves

- (1) Tuning the proportional gain. Increase the gain until the antenna hits the acceleration limits at typical commands and at expected disturbances.
- (2) Tuning the integral gain. Increase the gain until oscillations or undershoot appear. It should be smaller than the critical integral gain.

The proportional gain shapes the bandwidth of the transfer function T_{ry} . The larger the gain, the wider is the bandwidth. For a rigid antenna, the limit for the proportional gain is set by the antenna acceleration limits, since the increase of proportional gain increases antenna acceleration caused by commands and disturbances; see Figs. 6(c) and 6(d).

The integral gain shapes the disturbance transfer function at low frequencies. It is increased to obtain better disturbance rejection properties, but there is a limit to the increase: the integral gain should be smaller than the critical integral gain, i.e., should satisfy Condition (16), to prevent antenna oscillations.

IV. LQG Controller and a Flexible Antenna

Next, the LQG controller and flexible antenna are investigated. The closed-loop system has the same structure as in Fig. 2, except that the controller has the structure shown in Fig. 8 and the antenna model is a flexible structure model obtained from the system identification.

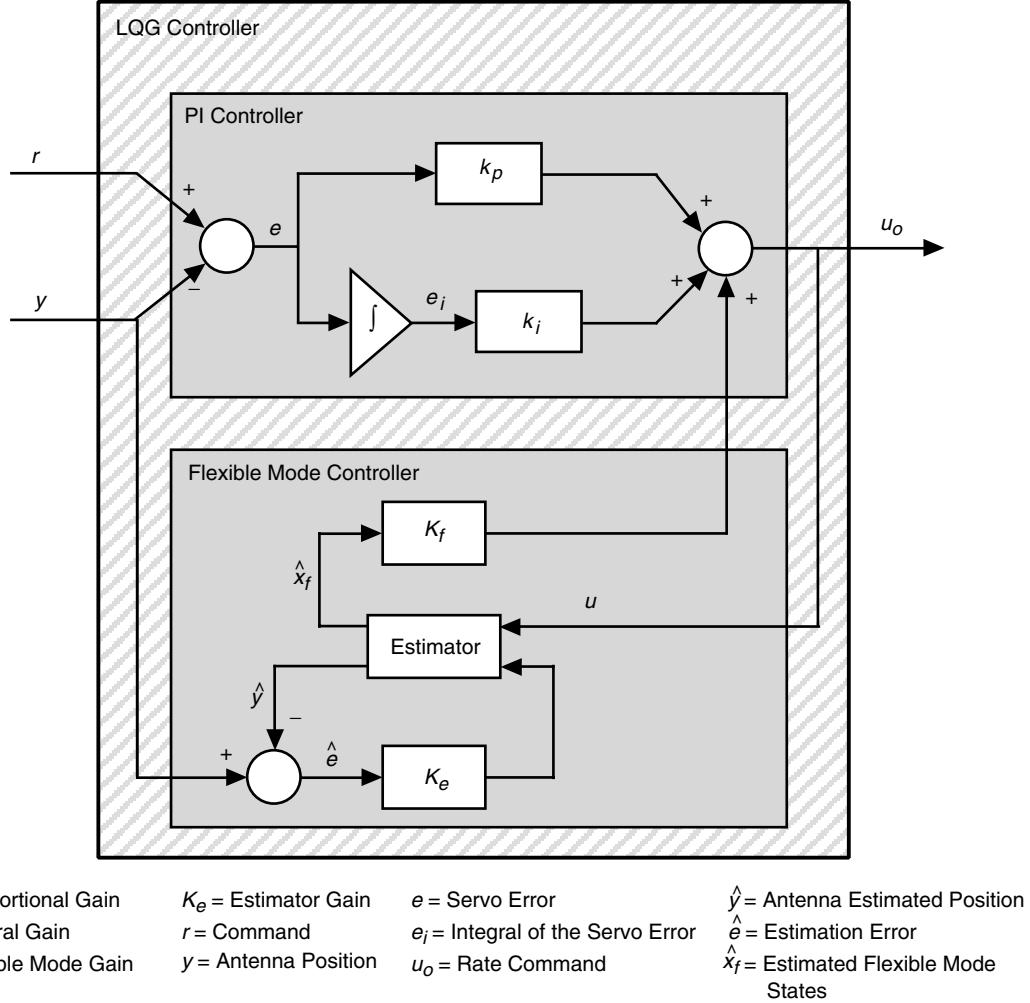


Fig. 8. LQG controller.

A. LQG Controller Description

The controller gains are obtained by minimizing the performance index J :

$$J^2 = E \left(\int_0^{\infty} (x_o^T Q x_o + u_o^T R u_o) dt \right) \quad (19)$$

In the above definition, Q is a positive semidefinite weight matrix and R is a positive scalar. We assume $R = 1$ since the case $R \neq 1$ is equivalent to $R = 1$ with the scaled weight matrix Q/R . The minimum of J is obtained for the feedback

$$u_o = -K_c \hat{x}_o \quad (20)$$

with the gain K_c obtained as

$$K_c = B_r^T S_c \quad (21)$$

and S_c is the solution of the controller algebraic Riccati equation

$$A_o^T S_c + S_c A_o - S_c B_o B_o^T S_c + Q = 0 \quad (22)$$

We see that the controller gain K_c depends solely on the weight matrix Q (A_o and B_o are fixed).

Similarly to the actual state x [see Eq. (5)], the estimated state consists of three components: estimated integral of the position \hat{y}_i , estimated position \hat{y} , and estimated flexible mode state \hat{x}_f :

$$\hat{x}_o = \begin{Bmatrix} \hat{y}_i \\ \hat{y} \\ \hat{x}_f \end{Bmatrix} \quad (23)$$

Correspondingly, the controller gain is divided into the proportional gain k_p , integral gain k_i , and flexible mode gain K_f , i.e.,

$$K_c = [k_i \quad k_p \quad K_f] \quad (24)$$

Introducing Eqs. (23) and (24) to Eq. (20), one obtains

$$u_o = -k_i e_i - k_p e - K_f \hat{x}_f \quad (25)$$

In the above equation, the antenna estimated position \hat{y} was replaced with the antenna servo error $e = r - y$, and the integral of the position was replaced with the integral of the servo error $e_i = \int e dt$ in order to turn a stabilizing controller into the tracking controller.

The missing part of the controller is the estimated state \hat{x}_o in Eq. (20). It is obtained from the estimator (which is a computer model of the antenna) as follows:

$$\dot{\hat{x}}_o = A_o \hat{x}_o + B_o u_o + K_e (y - C_o \hat{x}_o) \quad (26)$$

with the estimator gain given by

$$K_e = S_e C_o^T \quad (27)$$

and where S_e is the solution of the estimator algebraic Riccati equation

$$A_o S_e + S_e A_o^T - S_e C_o^T C_o S_e + V = 0 \quad (28)$$

For antenna controller tuning purposes, we assume $V = Q$ to obtain the balanced gains of the controller and the estimator; see [4].

B. LQG Weights in Modal Coordinates

In modal coordinates, the LQG weight matrix in Eq. (19) is selected as a diagonal matrix (due to the independence of states in modal coordinates), i.e.,

$$Q = \text{diag}(q_i, q_p, q_f) \quad (29)$$

where q_i is the integral weight, q_p is the proportional weight, and q_f is a vector of flexible mode weights. It is convenient to present the LQG weights in vector form as the LQG weight vector q :

$$q = \begin{Bmatrix} q_i \\ q_p \\ q_f \end{Bmatrix} \quad (30)$$

The weight vector q corresponds to the state vector x_r in Eq. (5), and the flexible mode weights are divided into weights of each mode:

$$q_f = \begin{Bmatrix} q_{f1m} \\ q_{f2m} \\ \vdots \end{Bmatrix} \quad (31)$$

with each mode weight $q_{fim}^T = \{q_{fi} \quad q_{fi}\}$ corresponding to the two-state mode.

For the antenna model in modal coordinates, the modal states are weakly coupled. They also are almost independent of the antenna position and integral of the position. Thus, the corresponding weights act independently on each flexible mode, and almost independently on position and on the integral of the position states. This adds to the flexibility of the controller tuning.

C. Resemblance of LQG and PI Controllers

Notice that for the rigid antenna the increase of the proportional gain improves antenna bandwidth and the disturbance rejection properties. However, an increase of proportional gain, when applied to a flexible antenna, is drastically limited: even a moderate gain can excite structural vibrations and cause instability; see [2]. However, the LQG controller consists of (besides the PI part) the flexible mode part (see Fig. 8), and the flexible mode controller is able to restrain antenna vibrations. In this way, the increased proportional gain does not excite vibrations and does not cause instability: a flexible antenna behaves approximately as a rigid one. Therefore, the controller tuning approach used for a rigid antenna with PI controller also can be used (with certain limitations) for tuning the LQG controller of a flexible antenna. The limitations are formulated as follows: the flexible mode gains should not be excessive; they should be large enough to assure vibration suppression, but not larger. Such a controller is called a low-authority LQG controller; see [4].

The following example shows the similarity between the rigid antenna with PI controller and the flexible antenna with LQG controller. Consider the 34-m antenna open-loop model with the transfer function from the rate input to the position output, shown in Fig. 4 (solid line). At lower frequencies, the transfer function is identical with the transfer function of an integrator, and at higher frequencies it shows flexible mode resonances. To this antenna we apply an LQG controller as follows. First, we select the weights of three LQG controllers such that their integral gain is zero and their proportional gains are 1, 4, and 16, respectively. For these cases, the plots of the magnitudes of the transfer functions T_{ry} , T_{wy} , T_{ra} , and T_{wa} are shown in Fig. 9. Comparing Fig. 9 and Fig. 6, we see similarities between the

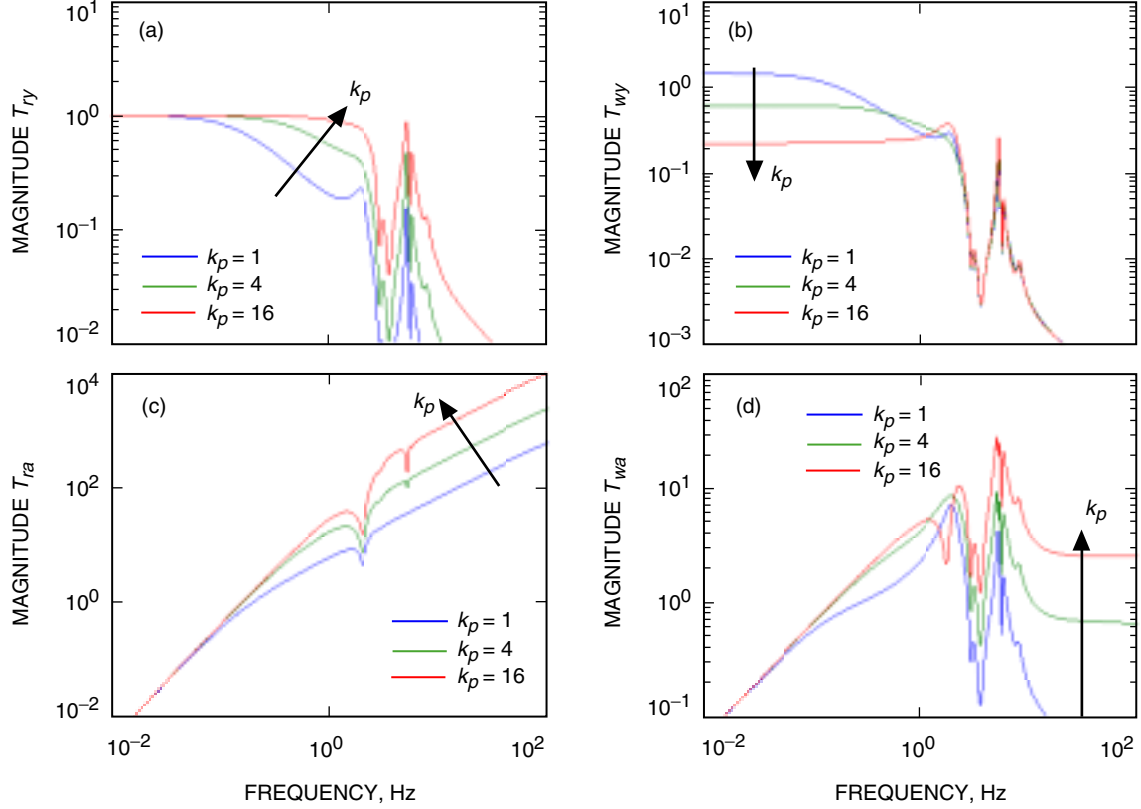


Fig. 9. Magnitudes of the transfer functions of the LQG controller, $k_i=0$: (a) T_{ry} , (b) T_{wy} , (c) T_{ra} , and (d) T_{wa} .

rigid antenna with PI controller and the flexible antenna with LQG controller. Namely, the plots of T_{ry} show the expanding bandwidth with the increase of the proportional gain. The plots of T_{wy} show the decreasing antenna response to disturbances with the increase of the proportional gain. The plots of T_{ra} and T_{wa} show increased acceleration response at high frequencies.

Next, we select the weights of the LQG controller to obtain a fixed proportional gain, $k_p = 16$, and to obtain the integral gains 1, 4, and 16, respectively. Note from Eq. (17) that the critical integral gain is 64 in this case. The plots of magnitudes of the transfer functions T_{ry} , T_{wy} , T_{ra} , and T_{wa} for the above three cases are shown in Fig. 10. Comparing Fig. 10 and Fig. 7, we see similarities between the rigid antenna with PI controller and the flexible antenna with LQG controller. The integral gain significantly impacts only the disturbance rejection properties (T_{wy}), and there is no significant impact on the closed-loop bandwidth (see the T_{ry} plot) and on the system acceleration (see the plots of T_{ra} and T_{wa}).

Finally, we analyze the impact of flexible mode weights on antenna dynamics. Figure 11 presents the magnitudes of the transfer functions T_{ry} , T_{wy} , T_{ra} , and T_{wa} for fixed proportional-and-integral gains ($k_p = 9.5$ and $k_i = 6.3$) and for small flexible mode weights (blue lines) and large flexible mode weights (green lines). The plots show that the excessive flexible mode weights reduce the closed-loop bandwidth, Fig. 11(a), and deteriorate the disturbance rejection properties, Fig. 11(b).

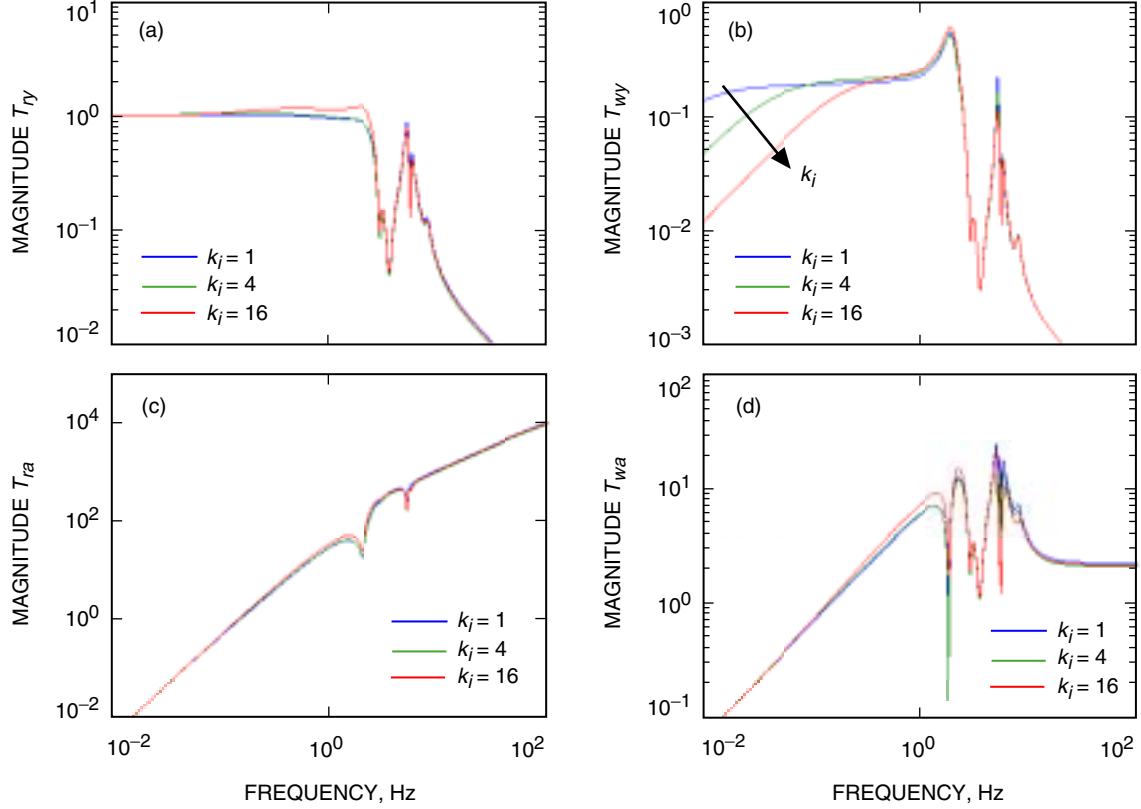


Fig. 10. Magnitudes of the transfer functions of the LQG controller, $k_p = 16$: (a) T_{ry} , (b) T_{wy} , (c) T_{ra} , and (d) T_{wa} .

D. Properties of the LQG weights

The above comparison shows that the LQG weights have an impact on a flexible antenna's performance similar to that of PI gains on a rigid antenna's performance, assuming the proper choice of coordinate system. The following list summarizes the properties of the LQG weights:

- (1) The increase of the flexible mode weights causes antenna vibration suppression. A single mode weight impacts only states corresponding to that particular mode (the flexible mode coordinates are weakly coupled).
- (2) The increase of the proportional weight increases the closed-loop bandwidth and improves the disturbance rejection properties.
- (3) The increase of the integral weight improves the disturbance rejection properties but does not impact the bandwidth.

The position and integral of the position weights are coupled, but they are easily manageable since the coupling involves two variables only.

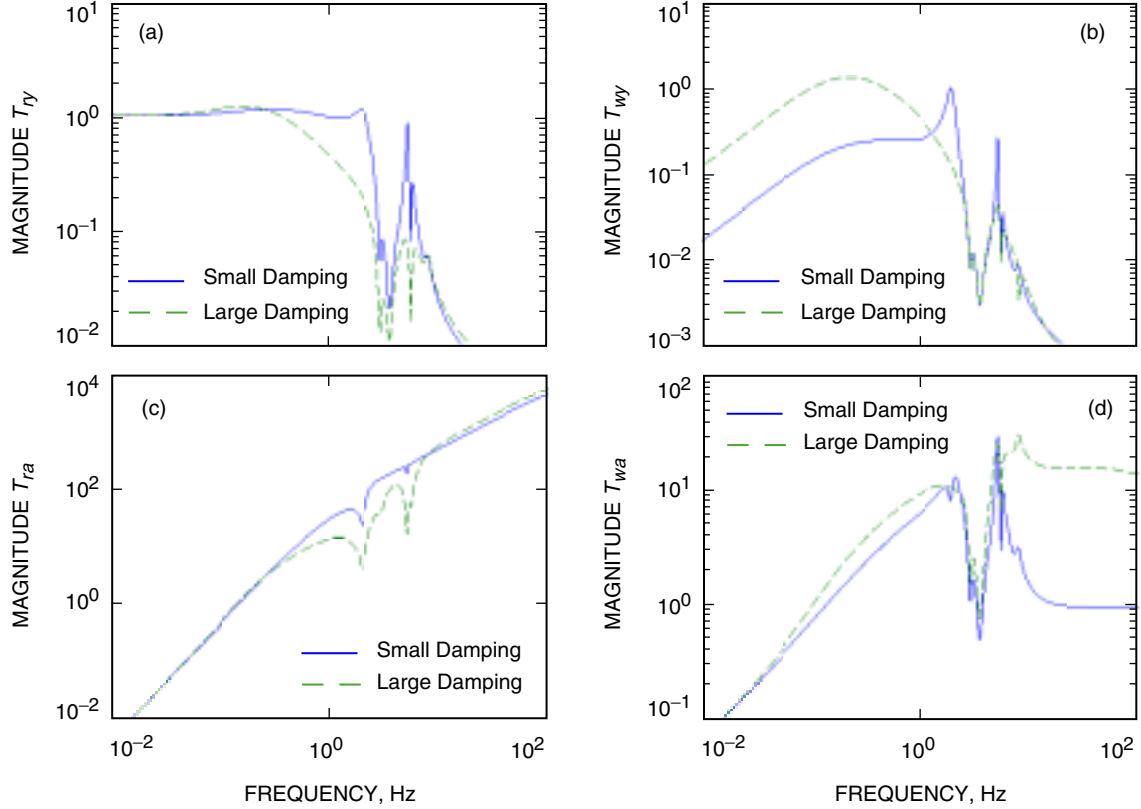


Fig. 11. Magnitudes of the transfer functions of the LQG controller for $k_p = 9.5$ and $k_i = 6.3$ for small flexible weights and large flexible weights, overdamped modes: (a) T_{ry} , (b) T_{wy} , (c) T_{ra} , and (d) T_{wa} .

E. Limits of the LQG Weights

The increases of the proportional, integral, and flexible mode gains have their limits, namely,

- (1) The increase of flexible mode weights should not be excessive. Large weights lead to overdamped dynamics and deteriorate overall antenna performance (reduced bandwidth, depreciated disturbance rejection properties).
- (2) The position weight is restricted by the antenna acceleration limit; large position weight causes excessive acceleration of the antenna that hits the acceleration limit and leads to nonlinear dynamics and deterioration of performance.
- (3) The integral weight should not exceed the critical integral gain in order to prevent low-frequency oscillations (these oscillations are lower than the antenna fundamental frequency).

F. LQG Controller Tuning Procedure

Based on the above analysis, the following sequence for LQG controller tuning is recommended:

- (1) Tuning the flexible mode weights. Apply small weights of the integral of the position and the position (which results in small PI gains), and also apply small flexible mode weights. Check the closed-loop transfer function for the appearance of flexible mode resonances. If they are excessive, increase the corresponding flexible mode weights. Do not apply unnecessarily large weights, since overdamped modes impact the antenna tracking performance.
- (2) Tuning the proportional weight. Increase the position weight; the proportional gain increases accordingly. The increase of the position gain causes the expansion of the closed-loop bandwidth. Increase the weight until bandwidth reaches the antenna fundamental frequency.
- (3) Tuning the integral weight. Increase the integral of the position weight, causing increase of the integral gain. The weight should increase until oscillations appear. The integral gain should satisfy Condition (16).
- (4) Correct the flexible mode weights. Check the flexible mode dynamics. If resonances resurface after tuning the proportional and integral parts, increase the corresponding flexible mode weights.

V. LQG Controller Tuning Tool

The procedure described above led to the development of the LQG controller tuning tool as a MATLAB[®] graphical user interface (GUI), shown in Fig. 12. The tool allows us to simulate antenna responses to step commands, disturbance steps, and wind gust disturbances. It also allows for manipulation of the LQG gains and observation of their impact on antenna performance. The performance is displayed in two windows: the upper-left window shows antenna responses to the command step and to the disturbance step; the upper-right window shows magnitudes of the command transfer function and disturbance transfer function. The numerical values of settling time [s], overshoot [%], steady-state error in the rate offset [mdeg], bandwidth [Hz], rms servo error in wind gusts [mdeg], and maximal value of the antenna response to unit step disturbance [deg] are displayed in the lower right box.

The LQG controller weights are adjusted using slides, which include a proportional weight slide, an integral weight slide, and flexible mode weight slides (marked at the tool as frequency weights). Thus, a user can manipulate the antenna performance by moving the weight slides and observing the antenna performance in the windows and in the right box. The tuning process is illustrated in [8].

VI. Conclusions

The article shows how to select the coordinates of the controller for simple tuning of the PI and LQG controllers. Also, it shows how the controller gains of the PI controller and the controller weights of the LQG controller impact the antenna closed-loop performance. Finally, it shows the limits of the LQG weights. These features make it possible to improve antenna performance in wind disturbances.

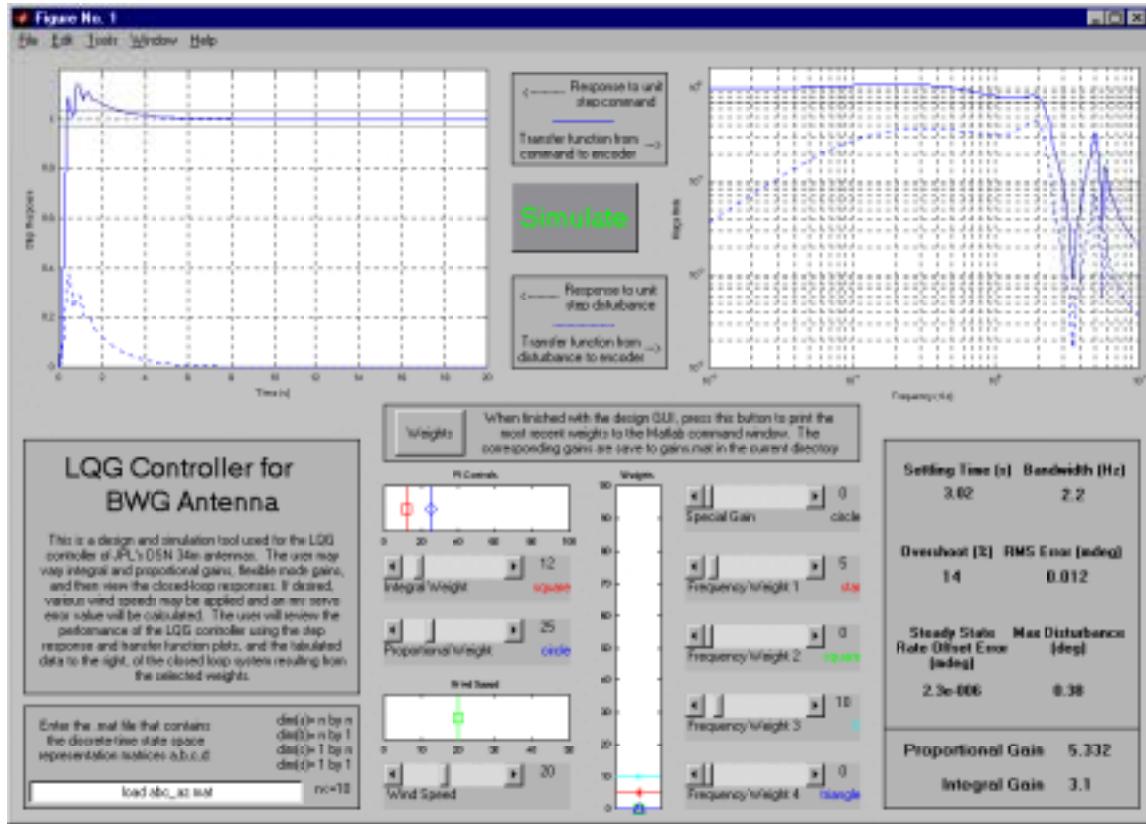


Fig. 12. The GUI of the antenna LQG controller tuning tool.

References

- [1] W. Gawronski, "Antenna Control Systems: From PI to H_∞ ," *IEEE Antennas and Propagation Magazine*, vol. 43, no. 1, pp. 52–60, 2001.
- [2] W. Gawronski, C. Racho, and J. Mellstrom, "Application of the LQG and Feed-forward Controllers for the DSN Antennas," *IEEE Transactions on Control Systems Technology*, vol. 3, pp. 417–421, December 1995.
- [3] W. Gawronski and K. Souccar, "Control Systems of the Large Millimeter Telescope," *Proceedings of the SPIE Conference on Astronomical Telescopes and Instrumentation*, Glasgow, United Kingdom, in press, 2004.
- [4] W. Gawronski, *Advanced Structural Dynamics, and Active Control of Structures*, New York: Springer, 2004.
- [5] C. D. Johnson, "Optimal Control of the Linear Regulator with Constant Disturbances," *IEEE Transactions on Automatic Control*, vol. 13, pp. 416–421, 1968.
- [6] M. Athans, "On the Design of PID Controllers Using Optimal Linear Regulator Theory," *Automatica*, vol. 7, pp. 643–647, 1971.

- [7] B. Porter, "Optimal Control of Multivariable Linear Systems Incorporating Linear Feedback," *Electronic Letters*, vol. 7, pp. 170–174, 1971.
- [8] E. Maneri and W. Gawronski, "LQG Controller Design Using GUI: Application to Antennas and Radio-Telescopes," *ISA Transactions*, vol. 39, pp. 243–264, 2000.